Symbol Frame Synchronization Technique for OFDM Burst Mode Transmission

Ki Yun Kim[1], Jun Yeob Lee[2], Hyung Jin Choi[2], and Ho Kim[1]
[1] R&D Team, Samsung-Thales, Giheung-Eup, Yongin-City, Korea
Tel. +82-19-339-5129, Fax.: +82-31-280-1620
[2] Commsys Lab, Department of Information and Communications Engineering,
Sungkyunkwan University, Suwon-City, Korea
e-mail : kiyunkim@samsung.co.kr, hjchoi@ece.skku.ac.kr

Abstract: In this paper, we propose a new frame structure and frame synchronization algorithm for OFDM burst mode transmission. On the contrary to conventional OFDM symbol based methods, the proposed preamble for symbol frame synchronization is designed independently in time domain in arbitrary length and is placed at the beginning of the frame. The proposed frame synchronization algorithm by using the preamble is working independent of frequency offset and robust to serious channel environment.

1. Introduction

OFDM is becoming increasingly popular in communication system design since it is bandwidth-efficient and is robust to multipath channel. Among the many applications of OFDM technique, OFDM burst mode communication is recently gaining wide interest in indoor as well as outdoor environment [1], [2].

Design of frame structure for OFDM burst mode communication must be considered with fast and accurate symbol frame start detection in the preamble area. In this paper, we propose a novel frame design structure and corresponding symbol frame start detection algorithm for OFDM burst mode transmission.

Symbol frame start detection in OFDM burst mode is equivalent to the symbol timing recovery for finding the correct position of the Fast Fourier Transform (FFT) window [3]~[6]; in this paper, we will call it the symbol frame synchronization. Symbol frame synchronization is firstly achieved by OFDM burst mode receiver when frequency offset and unequalized channel still remains. Thus, symbol frame synchronization must be robust to the frequency offset and the channel environment. Most of the conventional symbol frame synchronization algorithm was based on correlation between Guard Interval (GI) and rear part of symbol [3]~[5]. But these algorithms have problem that they cannot detect accurate symbol start position owing to the ISI in multipath fading channel.

The proposed symbol frame synchronization algorithm can effectively overcome these problems. On the contrary to conventional OFDM symbol based methods, which have fixed OFDM symbol size, our proposed algorithm detects symbol frame start position by using FSC (Frame Synchronization Code) signal of which the length can be variable in the time domain. The proposed symbol frame synchronization algorithm is also independent of the frequency offset and robust to serious channel environment by designing the length of FSC to be longer. Detailed description of the algorithm will be presented in the following Sections.

2. OFDM Burst Mode Transmission

2.1 Frame Structure and Signal Description

Proposed OFDM frame structure for burst mode communication can be divided into FSC area for symbol frame synchronization and data area for OFDM symbol transmission as shown in Fig. 1. The transmitted burst OFDM frame signal can be expressed as

$$S_{frame}(t) = S_{FSC}(t) + S_{data}(t - T_{FSC}) \tag{1}$$

where, T_{FSC} express the time interval of the FSC signal.

The proposed process of OFDM burst mode transmission is as follows. At transmitter, the generated digital sample sequence consists of the FSC, $C^A(n)$, samples prepared directly in time domain as will be given in Section 2.2 and data samples without GI produced by IFFT as shown in Eq. (2).

$$\begin{cases} s(n) = C^A(n) & n = 1,2,\cdots,C_L : for\ FSC \\ s_m(n) = \dfrac{1}{N}\displaystyle\sum_{k=0}^{N-1} X_m(k) e^{j\frac{2\pi nk}{N}} & k = 0,1,\cdots,N-1 : for\ data \end{cases} \tag{2}$$

Here, C_L means the sample or bit length of FSC, and FSC samples $C^A(n)$ are directly applied to the first $s(n)$ of the start of frame. $s_m(n)$ means sample sequence of the m-th OFDM symbol in time domain which is not added GI yet. $X_m(k)$ is the m-th complex transmit symbol in frequency domain, and N is the number of subcarriers.

2.2 FSC Generation

Proposed symbol frame synchronization algorithm is based on time domain preamble segment called FSC which is placed at the beginning of preamble, contrary to the conventional methods of using time domain samples out of the IFFT block.

FSC vector $C(n) = \{C(1), C(2), C(3), \cdots, C(C_L)\}$ consists of C_L binary values. For the code vector $C(n)$ with value 1, we perform alternative polarity inversion to make them into 3-level signal $C^A(n)$. For example, if $C(n) = \{1,0,0,1,1,1,0,1,\ldots\}$, then it becomes a 3-level signal $C^A(n) = \{1,0,0,-1,1,-1,0,1,\ldots\}$. By this procedure, we can maintain the number of 1 and -1 equally at the transmitter to eliminate the DC offset and maintain a certain level of dynamic range. In this paper, we adopted a PN code with length 127 to satisfy the required frame loss probability.

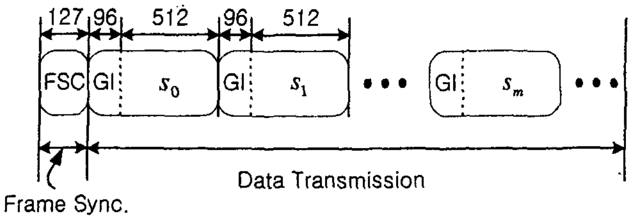

Fig. 1 Proposed OFDM burst mode frame structure

The FSC so designed is multiplied by the normalization constant $\sqrt{P}$ and is transmitted to I channel and Q channel simultaneously. If we assume the normalized symbol power of the 512 point IFFT output samples to be 1, FSC must have the normalized power of 127/512 since the length of FSC corresponds to 127/512 of the OFDM symbol. Because there are 64 of value $\pm\sqrt{P}$ and 63 of value 0 in FSC for both I channel and Q channel respectively, a total number of 128 $\sqrt{P}$ are transmitted in the both channel. Therefore, normalization constant $\sqrt{P}$ becomes $\sqrt{(127/512)\times(1/128)} \cong 0.044$.

3. OFDM Burst Mode Reception

3.1 FSC(Frame Synchronization Code) Detection

The symbol frame synchronizer in Fig. 2 consists of power detector, 0/1 detector, C_L number of shift registers, modified Modulo-2 adder, summation, and peak detector. The first thing to be done in the symbol frame synchronizer is to detect the power by using each received sample. If we assume the i-th optimal signal sample sequence after multipath channel and AWGN as $\tilde{s}(i)$, we can express a signal with frequency and phase offset into separate I and Q channel as in Eq. (3).

$$\begin{aligned} y(i) &= (\tilde{s}_I(i) + \tilde{s}_Q(i))e^{j\Theta} \\ &= (\tilde{s}_I(i)\cos\Theta - \tilde{s}_Q(i)\sin\Theta) + j(\tilde{s}_Q(i)\cos\Theta + \tilde{s}_I(i)\sin\Theta) \end{aligned} \tag{3}$$

Here, $\tilde{s}_I(i)$ and $\tilde{s}_Q(i)$ each means the I channel and Q channel of $\tilde{s}(i)$ and Θ expresses the total phase $2\pi i\varepsilon/N+\theta_0$ including frequency offset($\varepsilon=\Delta f T$) and phase offset(θ_0). If we perform power detection to the above sample sequence for symbol frame synchronization as in Fig. 2, we can obtain the power that is independent of frequency offset and phase offset as shown below.

$$y_I^2(i) + y_Q^2(i) = \tilde{s}_I^{\,2}(i) + \tilde{s}_Q^{\,2}(i) \tag{4}$$

3.2 Decision of Threshold Th_1

In what follows, we will derive analytically an optimum threshold Th_1 in AWGN environment to determine 0 and 1 from Eq. (4). It is very difficult to derive an optimum threshold in the multipath environment since it depends on FSC pattern. If we assume AWGN channel environment only, we can separately express the I channel and Q channel from Eq. (3) as

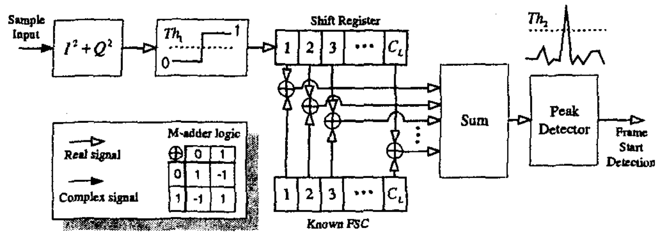

Fig. 2 FSC synchronization structure

$$\begin{cases} y_I(i) = (s_I(i)\cos\Theta - s_Q(i)\sin\Theta) + \eta_I(i) \\ y_Q(i) = (s_Q(i)\cos\Theta + s_I(i)\sin\Theta) + \eta_Q(i) \end{cases} \tag{5}$$

where, the additive terms $\eta_I(i)$ and $\eta_Q(i)$ are Gaussian random variables with zero mean and $\sigma_\eta^{\,2}$ variance.

For the I channel and Q channel of the transmitted FSC pattern, we will let a signal set like $\{ C^A{}_I(n), C^A{}_Q(n) \}$ = {0,0} to be S_1 and a signal set like $\{ C^A{}_I(n), C^A{}_Q(n) \}$ = $\{ \pm\sqrt{P}, \pm\sqrt{P} \}$ to be S_2. For each case of S_1 or S_2 transmission, power detection can be expressed as shown in Eq. (6) and Eq. (7), respectively.

$$y_I^2(i) + y_Q^2(i) = \eta_I(i)^2 + \eta_Q(i)^2 \tag{6}$$

$$\begin{aligned} y_I^2(i) + y_Q^2(i) = &[(\pm\sqrt{P}\cos\Theta \mp \sqrt{P}\sin\Theta) + \eta_I(i)]^2 \\ &+[(\pm\sqrt{P}\cos\Theta \pm \sqrt{P}\sin\Theta) + \eta_Q(i)]^2 \end{aligned} \tag{7}$$

Therefore, error probability of Eqs. (6) and (7) follows a central chi-square distribution and noncentral chi-square distribution of the degree of freedom n=2 [7]. The error probability of each can be expressed as shown in Eqs. (8) and (9), respectively.

$$\Pr\{e \mid S_1\} = \int_{Th_1}^{\infty} \Pr(z \mid S_1)dz = \int_{Th_1}^{\infty} \frac{1}{2\sigma_\eta^2} e^{-z^2/2\sigma_\eta^2} dz \tag{8}$$

$$\Pr\{e \mid S_2\} = \int_{-\infty}^{Th_1} \Pr(z \mid S_2)dz = \int_{-\infty}^{Th_1} \frac{1}{2\sigma_\eta^2} e^{-(2P+z)/2\sigma_\eta^2} I_0\!\left(\frac{\sqrt{2Pz}}{\sigma_\eta^2}\right) dz \tag{9}$$

Where, $I_\alpha(x)$ is the α -th order modified Bessel function.

Although the transmit probability of S_1 and S_2 each (63/127) and (64/127), we will simplify to set them equally at 1/2 for easy derivation of optimal threshold Th_1, and the total error probability $\Pr_{total}$ can be obtained as follows.

$$\Pr_{total} = \frac{1}{2}\int_{Th_1}^{\infty} \frac{1}{2\sigma_\eta^2} e^{-z^2/2\sigma_\eta^2} dz + \frac{1}{2}\int_{-\infty}^{Th_1} \frac{1}{2\sigma_\eta^2} e^{-(2P+z)/2\sigma_\eta^2} I_0\!\left(\frac{\sqrt{2Pz}}{\sigma_\eta^2}\right) dz \tag{10}$$

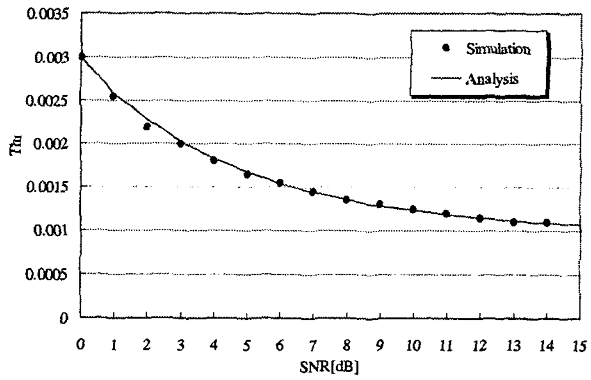

Fig. 3 Optimum threshold for Th_1 for various SNR

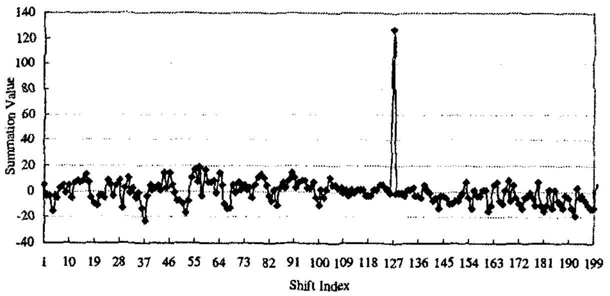

(a) SNR=10dB

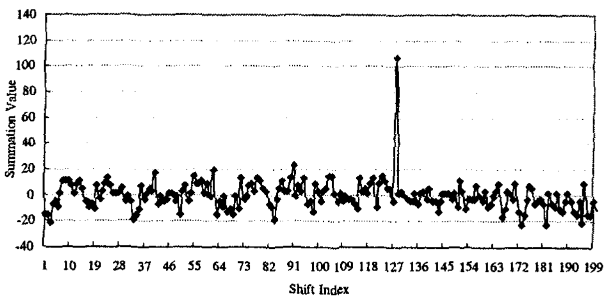

(b) 2nd path delay = 2μ sec, gain = -6dB

Fig. 4 Characteristics of peak detection correlation

To obtain the Th_1 value that minimizes the $\Pr_{total}$ we differentiate Eq. (10) with respect to Th_1 and obtain the optimal Th_1 that can make the derivative of Eq. (10) to be 0. Then the optimum threshold Th_1 can be obtained as,

$$Th_1 = \frac{\sigma_\eta^4}{2P}\{I_0^{-1}(e^{P/\sigma_\eta^2})\}^2 \tag{11}$$

where $I_0^{-1}(\cdot)$ is the inverse function of $I_0(\cdot)$.

Fig. 3 is a comparison between simulated and analytic (through Eq. (11)) value of optimum threshold Th_1 for different SNR. The optimum threshold value Th_1 tends to decrease for increased SNR and a good match between analytic and simulation result can be confirmed from this figure.

The values 0 and 1 so determined are input to the shift register of the FSC detector in accordance with the sample rate T_S and modulo-2 adder operation is performed C_L times with the known FSC pattern. Here, Modified modulo-2 adder outputs 1 if the bits are the same in the current position and outputs -1 if otherwise. These correlation values are all summed in the summation block and the result is compared with the Peak detector's threshold Th_2 to decide the FSC detection.

Fig. 4 depicts the output characteristics of the Peak detector based on the channel environment of the proposed system. The threshold is set to $Th_1 = 0.00125$. Fig. 4(a) is the case with only AWGN and when SNR=10dB, the maximum peak output was 127. On the other hand, Fig. 4(b) is not only for AWGN and SNR=10dB but also for multipath channel environment. For convenience, we assumed the two path multipath channel. The relative delay and gain of the delayed 2nd path to the 1st path are set to 2 μsec and -6dB, respectively. In Fig. 4(b), maximum peak output was 107. This value is reduced by 20 from the maximum peak of 127, which means that 10 sample errors occurred out of the received FSC region. This means that since the channel error probability in multipath channel increases sharply compared with the AWGN channel, we have to be very careful in selecting Th_1.

3.3 Decision of Threshold Th_2

If the true peak value out of the Peak detector is smaller than the threshold Th_2 that is set for peak detection, FSC cannot be detected. This is called the Missed detection probability P_M. On the other hand, if we set Th_2 too much low, correlation output out of other data area may accidentally go over Th_2 and is considered as FSC. This is called the False alarm probability P_F.

For symbol frame synchronization, missed detection probability, P_M can be obtained from P_C (Correct detection probability). P_C is the probability to detect FSC when the number of bit errors in the FSC becomes the same or less than the maximum error count ε (where $\varepsilon = (C_L - Th_2)/2$) that is allowed for peak detection. First, the probability of j bit errors among C_L number of FSC bits is as follows.

$$P(j) = \binom{C_L}{j} \Pr_{total}^{j} (1-\Pr_{total})^{C_L - j} \tag{12}$$

Therefore, correct FSC detection probability P_C can be obtained by adding the probability of FSC bit errors that are below error threshold ε as given by

$$P_C = \sum_{j=0}^{\varepsilon} P(j) \tag{13}$$

Missed detection probability P_M can be obtained by subtracting all correct detection probabilities out of total probability(=1).

$$P_M = 1 - P_C = 1 - \sum_{i=\varepsilon+1}^{C_L} \binom{C_L}{j} \Pr_{total}^{j} (1-\Pr_{total})^{C_L - j} \tag{14}$$

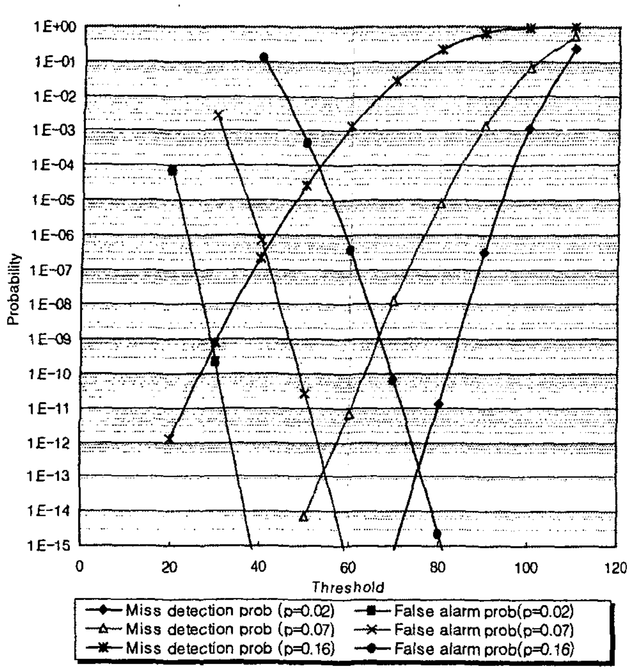

Fig. 5 Frame loss probability (W=50)

As error threshold ε is increased and FSC length C_L is increased, missed detection probability is decreased.

False detection probability P_F can be obtained as follows. If we assume FSC length to be C_L bits, all possible combinations of random data is 2^{C_L}, and if $\varepsilon=0$, false detection probability is $1/2^{C_L}$, which is the probability that random data combinations exactly match the FSC pattern. For a given value of ε, the total number of possible combinations in which ε or fewer errors can occur is $\sum_{j=0}^{\varepsilon}\binom{C_L}{j}$. Thus P_F can be given by

$$P_F = \frac{1}{2^{C_L}} \sum_{i=0}^{\varepsilon} \binom{C_L}{j} \tag{15}$$

and is independent of the average bit error probability $\Pr_{total}$ From Eq. (15), we can know that P_F can be reduced by increasing the number of FSC bits C_L or decreasing the detection threshold ε. Therefore, P_M and P_F can be traded against each other for fixed C_L by varying ε (or Th_2) value.

From the above Eqs. (14) and (15), P_M are very small and P_F are very high in general. This can be overcome by window (aperture) technique [8]. In window technique, FSC detection only within a particular interval with high expectation is considered as a peak, which is relatively simple and yields good performance.

Fig. 5 depicts P_M and windowing P_F, P_F^W. As mentioned previously, depending on Th_2 threshold, both probabilities are on a trade off relations. For false alarm probability, applying window technique improves performance. Also, P_F^W and P_M decrease as $\Pr_{total}$ decreases. If we assume the 2nd path gain to be not higher than -6dB, then both P_F^W and P_M can be expected to be below BER=10^{-2}.

As we mentioned previously, the proposed burst mode OFDM symbol frame synchronization algorithm can select the length and pattern of FSC, which is dependent on the channel environment and system performance requirements Thus, when channel environment is bad, we can extend the length of FSC to reduce P_F^W and P_M.

4. Conclusion

In this paper, we proposed frame architecture and symbol frame synchronization algorithm for OFDM burst mode communication. The proposed algorithm was independent of the frequency offset and robust to the multipath channel environment. In implementation, whereas conventional methods used the correlation outcomes to detect the symbol frame start position, the proposed method is simply based on a modified modulo-2 logic operation. The proposed scheme required setting of the optimum thresholds Th_1 and Th_2 for enhancing the symbol frame start detection probability, and the best strategy was to set them according to the most serious multipath channel environment. In the example system design, the FSC consists of 127 bits and assuming the channel environment with average BER of 0.07, we could obtain the frame loss probability of 10^{-13}. Note that we can also enlarge or shorten the length of FSC depending on the channel environment. We believe that these results are expected to contribute to communication frame design for burst mode OFDM.

References

[1] R. Van Nee, "A New OFDM Standard for High Rate Wireless LAN in the 5 GHz Band," *in Proc. IEEE VTC'99-Fall*, Vol. 1, pp. 258-262, Amsterdam, Netherlands, Sept. 1999.

[2] IEEE 802.11, *IEEE Standard for Wireless LAN Medium Access Control and Physical Layer Specifications*, Sept. 1999.

[3] J.-J. Van de Beek, M. Sandell, and P. O. Borjesson, "ML Estimation of Time and Frequency Offset in OFDM Systems," *IEEE Trans. Signal Processing*, Vol. 45, pp. 1800-1805, July 1997.

[4] B. Yang, K. B. Letaief, R. S. Cheng, and C. Zhigang, "Timing Recovery for OFDM Transmission," *IEEE J. Selec. Areas Commun.*, Vol. 18, no. 11, 2278-2291, Nov. 2000.

[5] T. M. Schmidl and D. C. Cox, "Robust Frequency and Timing Synchronization for OFDM," *IEEE Trans. Commun.*, Vol. 45, pp. 1613-1621, Dec. 1997.

[6] D. K. Kim, S. H. Do, H. B. Cho, H. J. Choi, and K. B. Kim, "A New Joint Algorithm of Symbol Timing Recovery and Sampling Clock Adjustment for OFDM Systems," *IEEE Trans. Consumer Electron.*, Vol. 44, no. 3, pp. 1142-1149, Aug. 1998.

[7] J. G. Proakis, *Digital Communications*, 3rd ed., McGraw-Hill, 1995.

[8] Tri T. Ha, *Digital Satellite Communications*, McGraw-Hill, 1990.